Stivala, S. (1977) *Fed. Proc., Fed. Am. Soc. Exp. Biol. 36*, 83–88.
Sturzebecher, J., & Markwardt, F. (1977) *Thromb. Res. 11*, 835–846.
Teien, A., & Abildgaard, U., & Höök, M. (1976) *Thromb. Res. 8*, 859–867.
West, S., Hurst, R., & Menter, J. (1977) *Biopolymers 16*, 685–693.

Copper(II) Protoporphyrin IX as a Reporter Group for the Heme Environment in Myoglobin†

Kenneth Alston‡ and Carlyle B. Storm*

ABSTRACT: Copper(II) protoporphyrin IX has been introduced into apomyoglobin, and its utility as a reporter group of the heme environment has been examined. The Soret and visible absorption bands and electron spin resonance spectrum show that the Cu(II) is five coordinate, probably through coordination to the F-8 proximal histidine. The resonance Raman spectrum does not indicate any appreciable distortion from the solution conformation of copper(II) protoporphyrin IX dimethyl ester in CS_2. The ultraviolet circular dichroism shows no alteration of the helical content of the globin from that of metmyoglobin. The circular dichroism of the porphyrin transitions suggests that the packing of the amino acid side chains around the porphyrin is different than that in the native metmyoglobin.

A variety of metalloporphyrins have been used as reporter groups for the immediate porphyrin environment in heme proteins. In myoglobin substituted with various metalloprotoporphyrin IX derivatives, the most thoroughly studied are those in which cobalt (Hoffman & Petering, 1970; Hoffman et al., 1971; Chien & Dickinson, 1972; Yonetani et al., 1974; Yamamoto et al., 1974; Hoffman & Gibson, 1978) and zinc (Andres & Atassi, 1970; Hoffman, 1975) have been substituted for iron. To a lesser degree silver, copper, manganese, nickel, chromium, ruthenium, rhodium, and ytterbium (Atassi, 1967; Andres & Atassi, 1970; Yonetani & Scrivastaua, 1974; Hoffmann & Gibson, 1978; Horrocks et al., 1975) have been studied.

The ideal reporter group with which to study the native structure and function of a protein is an isotopic substitution, i.e., ^{13}C for ^{12}C (Jones et al., 1976). For studies relating structure to function, small, well-defined changes in structure accompanied by useful spectroscopic probes are desirable in reporter groups. For example, nitroxide spin-labeled protoheme has been used to study heme–protein interactions in several hemoproteins (Asakura et al., 1971).

A wide variety of copper porphyrins have been studied and characterized by a variety of physical and spectroscopic techniques. Both their coordination chemistry and stereochemistry are different from the iron(II) and iron(III) porphyrins. The copper(II) porphyrins provide several useful spectroscopic probes for the study of the immediate heme environment by UV–vis, ESR, CD, and resonance Raman methods.

We report here a study of the utility of copper(II) protoporphyrin IX as a reporter group for the heme environment in myoglobin.

Materials and Methods

Sperm whale metmyoglobin was obtained from Sigma Chemical Co. A 1% (w/v) solution of $Fe^{III}Mb$[1] was prepared in distilled water, and the small percentage of $Fe^{II}Mb$ present was oxidized by the addition of solid $CuCl_2$ (Breslow & Gurd, 1963). The copper ions were removed by exaustive dialysis against 0.01 M NaOAc, 0.002 M EDTA, and 0.07 M KCl, and the pH was adjusted to 5.6 with 1 M HOAc. Dialysis was continued with three to four changes of glass-distilled water and finally against 0.01 M phosphate buffer, pH 6.1. Any insoluble material was removed by centrifuging or filtering. The $Fe^{III}Mb$ solution was absorbed on a 5 × 16 cm carboxymethylcellulose column equilibrated with 0.01 M phosphate buffer, pH 6.1, and operated under the conditions described by Hardman et al. (1966). The main component, peak IV, was then concentrated to 100–200 mL by using a Millipore molecular separator and applied to a 2.5 × 90 cm Sephadex G-25 (coarse) column equilibrated with distilled water. The purified $Fe^{III}Mb$ was concentrated to a smaller volume and used within 7 days or lyophylized and stored at 0–5 °C.

The heme group was removed from $Fe^{III}Mb$ by the procedure of Teale (1959) using 2-butanone, and apoMb was further prepared by the method of Breslow (1964), with the following modification. The apoMb was dialyzed against several changes of glass-distilled water to remove excess ketone, dialyzed twice against $NaHCO_3$ (50 mg/L), dialyzed again against several changes of distilled water, centrifuged, and used within several days. The apoMb concentration was determined by the extinction coefficient of 15.8 mM cm^{-1} at 280 nm as reported by Stryer (1965).

PPDME was prepared from whole blood according to Grinstein (1947), and the purity was checked by the extinction coefficients reported by Falk (1964).

^{63}Cu isotope (99.89% ^{63}Cu, 0.11% ^{65}Cu) was purchased from the Union Carbide Corp., Oak Ridge National Laboratories, in the form of cupric oxide. The cupric oxide was converted to cupric acetate monohydrate by heating the oxide (200 mg)

† From the Department of Chemistry, Howard University, Washington, D.C. 20059. *Received March 7, 1979.* This work has been supported by grants from the National Institutes of Health (GM 05001 and GM 70586) and the National Science Foundation (GP 38497).

‡ Present Address: Laboratory of Chemical Biology, National Institute of Arthritis, Metabolism, and Digestive Diseases, National Institutes of Health, Bethesda, MD 20014.

[1] Abbreviations used: MMb, a metalloprotoporphyrin IX myoglobin; PP, protoporphyrin IX; PPDME, protoporphyrin IX dimethyl ester; TPP, *meso*-tetraphenylporphin; MesoDME, mesoporphyrin IX dimethyl ester; TNB, trinitrobenzene; ESR, electron spin resonance; CD, circular dichroism; Mes, 2-(*N*-morpholino)ethanesulfonic acid; IHP, inositol hexaphosphate; OEP, octaethylporphyrin; DBM, Debye-Bohr magnetons.

0006-2960/79/0418-4292$01.00/0

in glacial acetic acid (600 mL) to near boiling. The temperature was maintained until all of the oxide dissolved. The solution was filtered hot, and the acid was removed on a rotary evaporator. PPDME was added to the cupric acetate with the metal acetate in a 2:1 excess (w/w). This mixture was then dissolved in equal volumes of chloroform–acetic acid, refluxed for 1 h, and filtered hot, and the solvent was removed on a rotary evaporator. The [$^{63}Cu^{II}$]PPDME was dissolved in a small amount of $CHCl_3$ and chromatographed on silica gel (240 mesh) by using $CHCl_3$ as the eluant. The fractions were checked by visible absorption and pooled. The $CHCl_3$ was removed, and the [$^{63}Cu^{II}$]PPDME was recrystallized twice from a small volume of $CHCl_3$ and excess CH_3OH, filtered, and dried in a vacuum over P_2O_5. Anal. Calcd for $CuC_{36}H_{36}N_4O_4$ (Schwarzkopf Microanalytical Laboratory): C, 66.29; H, 5.56; N, 8.59. Found: C, 66.52; H, 5.67; N, 8.47.

[$^{63}Cu^{II}$]Mb was prepared by the addition of a twofold molar excess of [$^{63}Cu^{II}$]PP to the apoMb. The [$^{63}Cu^{II}$]PP was prepared by the basic hydrolysis of [$^{63}Cu^{II}$]PPDME. The weighed amount of [$^{63}Cu^{II}$]PPDME was dissolved in a minimum amount of pyridine, 1 volume of 1% KOH was added for every 3 volumes of pyridine, and the solution was heated gently with stirring for 2.5 h. The reaction was followed to completion by observing changes in the Soret band at 387 nm. The reaction mixture was allowed to cool and then added to a cold (5–10 °C) solution of apoMb in distilled water with gentle stirring. After addition to the [$^{63}Cu^{II}$]PP, the pH was adjusted to 8.0–8.5 with 1 M HCl, and the solution was left stirring in the cold overnight.

The Cu^{II}Mb was purified by adjusting the pH to 6.0, centrifuging to remove any precipitate, and applied to a 2.5 × 90 cm Sephadex G-25 (coarse) column equilibrated and eluted with glass-distilled water. The flow rate was 5 mL/min, and each fraction was checked by monitoring the Soret band at 425 nm. All pure fractions were pooled and purified further on carboxymethylcellulose according to Andres & Atassi (1970).

In order to determine the extinction coefficient of Cu^{II}Mb, we hydrolyzed samples of Fe^{III}Mb and Cu^{II}Mb, of known optical density at 280 nm, in 2 N mercaptoethanesulfonic acid for 24 h at 110 °C in evacuated sealed tubes according to the method of Penke et al. (1974). The amino acid analysis was obtained on a Beckman 118C amino acid analyzer using a single column. The extinction coefficient of Cu^{II}Mb was calculated relative to the known value of 3.17×10^4 for Fe^{III}Mb (Clark & Gurd, 1967) based on the comparison of the amino acids obtained in the two analyses. A molar extinction coefficient of 2.92×10^4 was calculated for Cu^{II}Mb.

TPP was synthesized according to the procedure of Adler (1967) and purified by the method of Barnett et al. (1973). [$^{63}Cu^{II}$]TPP was prepared by the same method that was described for [$^{63}Cu^{II}$]PPDME.

All of the pyridines (liquids) were purified by spinning band distillation, and the other basic compounds (solids) were purified by sublimation. The compounds were stored in the dark and kept cold.

ESR measurements were obtained on a Varian E-9 spectrometer operating at 9.5 GHz. Low-temperature studies (77 K) were carried out by using a quartz Dewar with the sample frozen in polyethylene Intramedic tubing. The various g values were calculated according to the method of Manoharan & Rogers (1969). CD experiments were carried out on a Cary Model 60 spectropolarimeter. Resonance Raman measurements were made in Professor T. Spiro's laboratory at Princeton University (Spiro & Strekas, 1974).

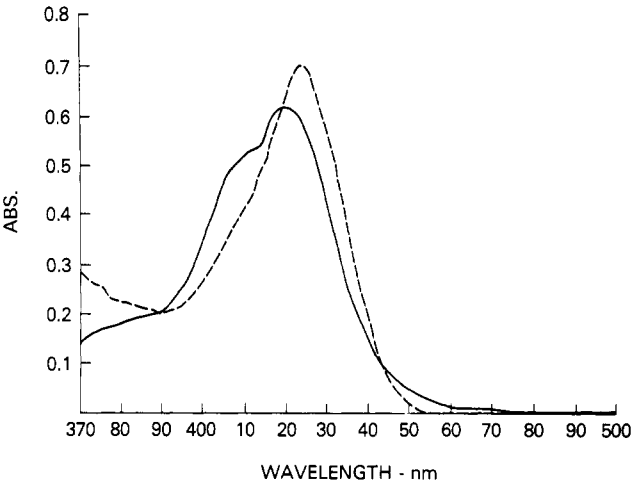

FIGURE 1: Soret band spectrum of Cu^{II}PPDME, 7×10^{-6} M in piperidine. (—) Room temperature; (---) −15 °C.

Table I: Position of the Soret Band in Cu^{II}TPP and Cu^{II}PPDME in Coordinating and Noncoordinating Solvents at 25 °C and at −15 °C

copper(II) porphyrin	ligand	Soret band at 25 °C (nm)	Soret band at −15 °C (nm)
Cu^{II}TPP	chloroform	415	415
	pyridine	420	423
	piperidine	426	427
	2-methylpyridine	418	419
Cu^{II}PPDME	chloroform	407	407
	pyridine	411	420
	piperidine	413, 422	425
	2-methylpyridine	410	411

Results and Discussion

Ultraviolet and Visible Studies of Cu^{II}PPDME, Cu^{II}TPP, and Cu^{II}Mb. The coordination of Cu^{II}PPDME and Cu^{II}TPP with extraplanar ligands was studied by using piperidine, pyridine, and 2-methylpyridine. The Soret band of Cu^{II}PPDME in piperidine at room temperature and −15 °C is shown in Figure 1. At room temperature two Soret bands are observed, one at 413 nm and the other at 422 nm. The short-wavelength band (413 nm) is associated with Cu^{II}PPDME being four coordinate while the longer wavelength band (422 nm) is associated with a five-coordinate copper complex (Baker et al., 1963a). Upon lowering the temperature to −15 °C, we observed marked changes. The two Soret bands at room temperature shift to a single Soret band at 425 nm. Similar results were obtained from Cu^{II}TPP as shown in Table I. It can be seen from the results listed in Table I that ligand complexation of Cu^{II}PPDME and Cu^{II}TPP with piperidine and pyridine is facilitated by lowering the temperature. No evidence for 2-methylpyridine binding to these Cu^{II}porphyrins was observed from the behavior of the Soret band at the temperatures covered. These results are similar to those reported for Cu^{II}MesoDME (Baker et al., 1963a).

The ultraviolet and visible spectra of Cu^{II}PP and Cu^{II}Mb are shown in Figure 2. From the results listed in Table II it is seen that large changes occur in the Soret band. These changes are best interpreted in comparison to the peaks observed with Cu^{II}PPDME in chloroform and pyridine (Falk, 1964) where the Soret band appears at 407 and 411 nm, respectively. Shifts in the positions of the α and β bands in

Table II: Peak Positions for the UV and Vis Spectra of $Cu^{II}PP$ and $Cu^{II}Mb$

porphyrin complex	solvent	wavelength (nm)					ref
$Cu^{II}PP$	10 mM Na_2HPO_4, 0.01% KCl	244	315	398	532	570	Atassi (1967)
$Cu^{II}Mb$	10 mM phosphate buffer, pH 7.0, 0.01% KCl	279	355–360	421	543		Atassi (1967)
$Cu^{II}PP$	pyridine			387	538	575	this work
$Cu^{II}PP$	0.05 M Mes buffer, pH 7.1, 0.05 M KCl		335	385	540	577	this work
$Cu^{II}Mb$	0.05 M Mes buffer, pH 7.1, 0.05 M KCl	279	350	425	545	585	this work

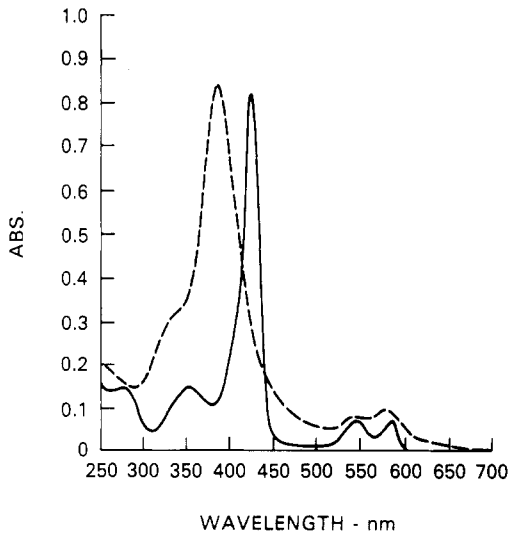

FIGURE 2: Ultraviolet and visible spectra of $Cu^{II}PP$ (---) and $Cu^{II}Mb$ (—) in 0.5 M Mes and 0.05 M KCl, pH 7.1.

the longer wavelength region also occur along with changes in the relative intensities of these bands (Nappa & Valentine, 1978).

The anions, azide, fluoride, cyanide, and thiocyanate, that are known to bind and cause spectral shifts in the ultraviolet and visible regions of $Fe^{II}Mb$ and $Fe^{III}Mb$ (Antonini & Brunori, 1971) were added to $Cu^{II}Mb$. No spectral changes were observed when these anions were added in a 100-fold excess.

$Cu^{II}Mb$ has been prepared by Atassi (1967) and shown by atomic absorption analysis to contain only one copper atom per protein molecule and to have an electrophoretic mobility identical with that of native $Fe^{III}Mb$. Atassi's results and the spectral studies reported here strongly support a specific 1:1 binding of $Cu^{II}PP$ to apoMb.

The ability of copper metalloporphyrins to form five-coordinate complexes with a variety of nitrogen bases has been reported (Miller & Dorough, 1952; Baker et al., 1963a,b, 1964). Numerous other metallo derivatives of the porphyrin ring system are also known to form higher coordinate complexes with ligands such as pyridine and imidazole. An important factor in the complexation of heme to globin in hemoglobin and myoglobin is the coordination of the imidazole side chain of histidine, and our results strongly suggest that this complexation is mimicked in $Cu^{II}Mb$ as well as in two model compounds.

$Cu^{II}PPDME$ and $Cu^{II}TPP$ were used as model compounds with square-planar symmetry with $Cu^{II}PPDME$ serving as the model compound most closely related to $Cu^{II}PP$, which is the porphyrin incorporated into apomyoglobin, forming $Cu^{II}Mb$. The coordination chemistry of $Cu^{II}PPDME$ is quite similar to that previously reported for $Cu^{II}MesoDME$ by Baker et al. (1963a). With $Cu^{II}PPDME$ in piperidine at room temperature, two Soret bands are observed (Figure 1). However, upon lowering the temperature to −15 °C only one Soret band is present at a longer wavelength than either of the two bands observed at room temperature (Figure 1). Normally the Soret band for a copper porphyrin in chloroform or pyridine occurs between 405 and 410 nm at room temperature. Decreasing the temperature of $Cu^{II}PPDME$ in chloroform to −15 °C does not affect the position of the Soret band whereas in pyridine or piperidine a significant red shift occurs. Baker et al. (1964) reported that a red shift in the Soret band of 10 nm is associated with the addition of one extraplanar ligand. That the Soret band of $Cu^{II}PPDME$ shifts 9 and 12 nm toward the red in pyridine and piperidine, respectively (Table I), demonstrates that $Cu^{II}PPDME$ is able to increase its coordination number from four to five. The complexation of $Cu^{II}TPP$ in pyridine and piperidine is nearly complete at room temperature (Miller & Dorough, 1952), so much so that the two Soret bands which were observed with $Cu^{II}PPDME$ in piperidine are not seen, and therefore only a small shift in the spectrum is observed when the temperature is lowered. However, the same conclusion can be made for $Cu^{II}TPP$ as for $Cu^{II}PPDME$ when the shifts are compared to that in chloroform. In pyridine and piperidine shifts of 8 and 12 nm are observed, respectively. The coordination geometry of the two model compounds studied here thus changes from a four-coordinate, square-planar complex to a five-coordinate, square-pyramidal complex.

Figure 2 shows the UV-visible spectra of $Cu^{II}PP$ in pyridine and $Cu^{II}Mb$ in Mes buffer. It can be seen that upon complex formation of $Cu^{II}PP$ with apoMb a major shift occurs in the Soret band along with changes in the relative intensities of the α and β bands. Correlation of the magnitude of the red shifts with the relative intensities of the α and β bands has been previously reported for a series of metalloporphyrins where the metal atom is changed (Gouterman, 1978, 1959). In those cases the α/β ratio decreases with the red shift for PP complexes and increases for TPP complexes. Gouterman et al. (1973) carried out extended Hückel calculations in order to estimate the electron densities on the metal, halide, and porphyrin ring in a series of $Sn(porph)X_2$, where X = F, Cl, Br, or I. Their results show the charge on the metal remaining relatively constant while increasing amounts of negative charge are transferred to the porphyrin ring in the order F < Cl < Br < I. They concluded that the effect on the spectrum of changing axial halides is similar to that observed upon changing metals in a series of closed-shell metalloporphyrins. In such a series it is observed that red shifts and α/β intensity ratio changes are correlated with the electronegativity of the metal. It is also suggested that decreasing electronegativity of the metal results in a shift of electron density from the metal toward the porphyrin ring. Complexation of ligands that donate charge to the metal is believed to have the same effect,

i.e., increase transfer of charge out onto the porphyrin ring.

Nappa & Valentine (1978) reported on a variety of neutral and anionic ligands complexed to $Zn^{II}TPP$. Their results clearly implicate charge as a factor in the red shift because all of the anion complexes are more red-shifted than the neutral ligand complexes. They also state that the red shift and α/β intensity ratio changes are derived from the amount of negative charge transferred from the ligand to the porphyrin via the Zn(II) atom. Thus, $Zn^{II}TPP$ preferentially binds "hard" ligands with donor atoms that have relatively high electronegativities and low polarizabilities such as N or O donor ligands while the ligands with less electronegative, more polarizable atoms such as S, P, or unsaturated N cause a larger red shift because they allow more negative charge to be transferred to the porphyrin ring.

In both $Cu^{II}TPP$ and $Cu^{II}PPDME$, piperidine causes a larger red shift in the Soret than pyridine. In $Cu^{II}Mb$, where we believe the fifth coordination site is occupied by the N atom of the imidazole group of the F8-histidine residue, the unsaturated N atom gives a red shift comparable to that of piperidine with $Cu^{II}PPDME$. This could also be due to the hydrophobic environment of the heme pocket or the deprotonation of the coordinated imidazole side chain of the F-8 histidine.

The results shown in Table II are similar to those reported by Atassi (1967). In addition, we have examined the effect of several anions (azide, fluoride, cyanide, and thiocyanate) on the visible and Soret spectrum. In no case did a 100-fold excess of the anion have any effect. Unlike the $Fe^{III}Mb$, it appears that the extraplanar coordination of the $Cu^{II}Mb$ is fully saturated by the F-8 histidine and maintains a square-pyramidal coordination even in the presence of a large excess of other potential ligands.

ESR of Copper(II) Porphyrins with Basic Ligands and $Cu^{II}Mb$. The ESR hyperfine and superhyperfine structure of $Cu^{II}TPP$ is well resolved in solution at room and low temperature (77 K), allowing calculation of the various ESR parameters. With strong-bonding ligands such as pyridine and piperidine, the average hyperfine splitting, $\langle A_{Cu} \rangle$, decreased from 96 G to approximately 90 G while the average nitrogen superhyperfine splitting, $\langle A_N \rangle$, decreased from 16 to 14 G upon ligand binding. The ESR of $Cu^{II}TPP$ at 77 K with different basic ligands followed the same pattern as the room-temperature spectra. The parallel hyperfine splitting, $A_{Cu(\|)}$, and the parallel superhyperfine splitting, $A_{N(\|)}$, decreased, while the $g_\|$ increased with strong-bonding ligands. The $B_{Cu(\perp)}$ decreased and the $g_\perp$ increased in a similar but much less distinct trend. Ligands which did not complex had spectral parameters very similar to those obtained for $Cu^{II}TPP$ in chloroform. If the $A_{Cu(\|)}$ values are plotted as a function of $g_\|$ by the method of Swartz et al. (1972) (Table III), a linear relationship is obtained for systems going from a four-coordinate complex to a five-coordinate complex.

The room-temperature ESR spectra of $Cu^{II}PPDME$ in chloroform, pyridine, and piperidine were found to be very similar to the spectra observed for $Cu^{II}TPP$. However, upon freezing the samples to 77 K, a broad signal was observed. These results are similar to those reported by MacCragh et al. (1965). Since a fivefold or greater excess of free-base PPDME was necessary in order to achieve a well resolved spectrum with $Cu^{II}PPDME$, the magnetic interaction of the free-base TPP with $Cu^{II}TPP$ was also studied. $Cu^{II}TPP$ in $CHCl_3$, benzene, and mixtures of chloroform–TPP and chloroform–TNB was studied at 77 K. With $Cu^{II}TPP$ in $CHCl_3$–TPP, small changes are seen when compared to the spectrum without TPP. The spectral lines are shifted about 3 G to the high-field part of the spectrum, and the well resolved $m = -1/2$ component seen in $CHCl_3$ is slightly masked by the perpendicular absorption. In $Cu^{II}TPP$ in $CHCl_3$–TNB, the lines are shifted approximately 5 G in the high-field direction. From the results in Table IVb, it can be seen that benzene, TPP, and TNB do indeed affect the anisotropic ESR parameters of $Cu^{II}TPP$ to a small degree, which we say more about below.

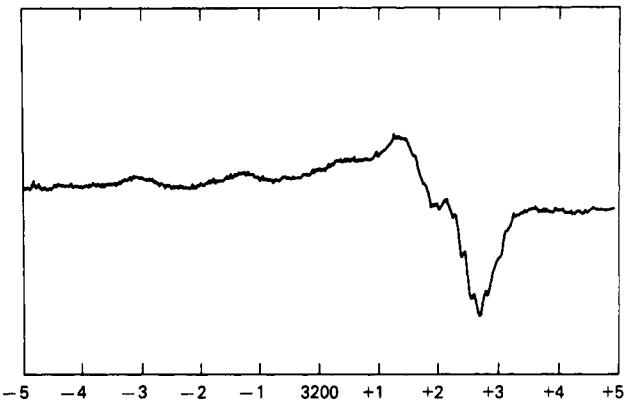

FIGURE 3: ESR spectrum of $Cu^{II}Mb$, 8×10^{-4} M at room temperature in H_2O. Scan range: 1000 G.

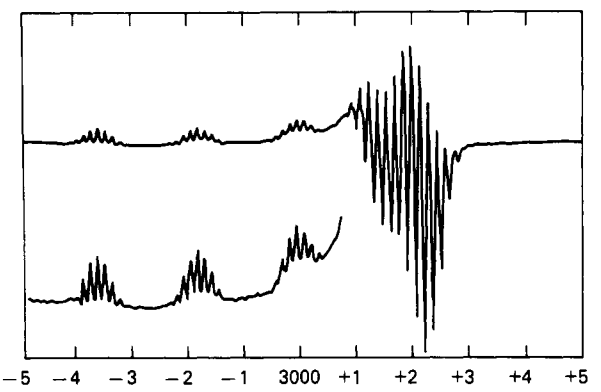

FIGURE 4: ESR spectrum of $Cu^{II}Mb$, 8×10^{-4} M at 77 K in 0.05 M Mes and 0.05 M KCl, pH 7.1. Scan range: 1000 G.

The room-temperature ESR spectrum of $Cu^{II}Mb$ is shown in Figure 3. The copper hyperfine lines in the parallel part are well resolved, and the usual large signal in the perpendicular region is resolved with some nitrogen superhyperfine splitting showing. Upon freezing the solution to 77 K (Figure 4), we found that the superhyperfine splitting due to the porphyrin nitrogens is clearly resolved in both the parallel and perpendicular components of the spectrum. The ESR parameters of $Cu^{II}Mb$ in solution at room temperature are nearly anisotropic but will be reported as average values, calculated from the 77 K spectrum, with $\langle g \rangle$ equal to 2.0775, $\langle A_{Cu} \rangle$ equal to 0.01722 cm^{-1}, and $\langle A_N \rangle$ equal to 0.00149 cm^{-1}. The ESR parameters of $Cu^{II}Mb$ at 77 K are given in Table III.

A number of copper(II) porphyrins have been studied and shown to be quite suitable for ESR examination (McGarvey, 1956; Assour, 1965; MacCragh et al., 1965; Bryce, 1966). The Cu(II) ion is of a d^9 configuration with one unpaired electron. The unpaired electron shows hyperfine interaction with the copper nucleus and superhyperfine interaction with the porphyrin nitrogens. In addition, the g values for the Cu(II) ion depend on the nature of the porphyrin substitution and the nature of the axial ligand which is coordinated to the copper atom. Thus, any change which affects the electron spin density at the Cu(II) or porphyrin N atom can be monitored by ESR

Table III[a]

[^{63}Cu]TPP and ligand	no.	$\langle g \rangle$	$g_{\parallel}$	$g_{\perp}$	$A_{Cu(\parallel)}$	$B_{Cu(\perp)}$	$A_{N(\parallel)}$	$B_{N(\perp)}$	ref
1-methylimidazole	1	2.1114	2.2253	2.0546	0.01860	0.00342	0.00135	0.00148	this work
4-vinylpyridine	2	2.1106	2.2252	2.0534	0.01891	0.00391	0.00135	0.00148	this work
3-methylpyridine	3	2.1099	212211	2.0544	0.01898	0.00277	0.00132	0.00158	this work
4-methylpyridine	4	2.1086	2.2193	2.0533	0.01886	0.00327	0.00129	0.00148	this work
2,6-dimethylpyridine	5	2.1002	2.2145	2.0431	0.01964	0.00430	0.00130	0.00178	this work
2,5-dimethylpyridine	6	2.1051	2.2124	2.0514	0.01947	0.00357	0.00129	0.00144	this work
pyridine	7	2.1057	2.2122	2.0524	0.01057	0.00270	0.00137	0.00144	this work
piperidine	8	2.1052	2.2108	2.0524	0.01982	0.00358	0.00127	0.00148	this work
2-methylpyridine	9	2.1139	2.2059	2.0679	0.02019	0.00392	0.00138	0.00159	this work
3-aminopyridine	10	2.0981	2.2030	2.0456	0.02016	0.00406	0.00135	0.00148	this work
2,4-dimethylpyridine	11	2.0928	2.1981	2.0402	0.01965	0.00400	0.00144	0.00167	this work
2-aminopyridine	12	2.0965	2.1968	2.0463	0.02067	0.00401	0.00142	0.00162	this work
2-vinylpyridine	13	2.0941	2.1938	2.0443	0.02064	0.00486	0.00143	0.00153	this work
chloroform	14	2.0859	2.1871	2.0354	0.02027	0.00432	0.00144	0.00152	this work
		2.0868	2.187_{63}	2.032_{63}	0.0209	0.00318	0.00144	0.00159	Manoharan & Rogers (1969)
			2.183_{65}	2.077_{65}	0.0209	0.00317	0.00144	0.00159	Manoharan & Rogers (1969)
		2.1073	2.187_{63}	2.067_{63}	0.0218	0.0039	0.00145	0.00164	Assour (1965)
			2.181_{65}		0.0218				Assour (1965)
2-acetylpyridine	15	2.0880	2.1811	2.0414	0.02144	0.00478	0.00143	0.00157	this work
copper myoglobin		2.0775	2.2230	2.0047	0.0185		0.00135	0.00138	this work
copper cytochrome *c*			2.216	2.050	0.01893	0.00182	0.00119	0.00139	Findlay et al. (1977)

[a] All hyperfine values are expressed in centimeters^{-1}. To convert gauss to centimeters^{-1} divide gauss by 21 418 and multiply by the corresponding *g* factor.

Table IV

solvent	$\langle g \rangle$	$g_{\parallel}$	$g_{\perp}$	$A_{Cu(\parallel)}$	$B_{Cu(\perp)}$	$A_{N(\parallel)}$	$B_{N(\perp)}$
		(a) CuPPDME plus PPDME and Solvent					
chloroform	2.09462	2.19787	2.04299	0.02037	0.00360	0.00144	0.00167
pyridine	2.08961	2.18887	2.03998	0.02059	0.00317	0.00141	0.00162
piperidine	2.09133	2.19166	2.04116	0.02077	0.00353	0.00143	0.00159
		(b) CuTPP and Solvent					
chloroform		2.0859	2.1871	2.0354	0.02027	0.00144	0.00152
benzene		2.0906	2.1901	2.0409	0.02045	0.00141	0.00157
chloroform and TPP		2.09073	2.19160	2.04030	0.02052	0.00143	0.00157
chloroform and TNB		2.08713	2.1860	2.03770	0.02056	0.00143	0.00162

spectroscopy. The ESR parameters, $g_{\parallel}$, $g_{\perp}$, $A_{Cu(\perp)}$, and $B_{Cu(\perp)}$ describe how the Cu(II) atom is being affected by complexing ligands while $A_{N(\parallel)}$ and $B_{N(\perp)}$ give information on how the spin densities at the nitrogens are being perturbed.

The $g_{\perp}$ ESR results of Cu^{II}TPP with basic ligands did not show any systematic variation in the ESR parameters. However, as can be seen in Table III, $g_{\parallel}$ and $A_{Cu(\parallel)}$ do vary in a rather systematic way. From these results it is clear that as $g_{\parallel}$ increases $A_{Cu(\parallel)}$ decreases. This is equivalent to saying that the in-plane ligand field strength of Cu^{II}TPP and Cu^{II}Mb decreases as the electron spin density at the Cu(II) center is removed by coordination of a fifth ligand. In substituted copper(II) deuteroporphyrins, it was found that $g_{\perp}$ varied in a systematic way with the σ_p of the substituent, in both chloronaphthalene and pyridine solvents (Baker et al., 1973). There was a shift of $g_{\perp}$ toward higher values, as well as a lowering of the nitrogen superhyperfine splitting, $A_{N(\parallel)}$, as the electron-withdrawing nature of the substituent increases.

The ESR results show that the environment of the Cu(II) center is being perturbed by the extraplanar ligands. This can be brought about in two ways. The extraplanar ligand can cause a change in electron distribution with little change in copper(II) porphyrin geometry, or the extraplanar ligand could cause a significant doming of the copper(II) porphyrin, with a movement of the Cu(II) from the plane of the porphyrin, in the same way as five-coordinate zinc(II) porphyrins (Hoard, 1975). A choice between these models cannot be made based on our ESR results.

The ESR spectra of copper porphyrins with highly electronegative groups or exocyclic rings attached to the periphery of the pyrroles show only a broad peak at 77 K in pyridine solvent (MacCragh et al., 1965). The hyperfine structure is regained when a small quantity of free-base porphyrin is added. In all cases the hyperfine structure is resolved at room temperature. We encountered the same problem when studying the ESR of Cu^{II}PPDME and Cu^{II}PP in the presence of basic ligands. Due to aggregation of these two complexes at 77 K, ESR data could not be obtained in the same way as with Cu^{II}TPP. The use of free-base PP and PPDME separates the molecules such that a well resolved ESR spectrum can be observed at both room temperature and 77 K; however, the π system of the free base was found to interfere with the binding of the basic compounds to Cu^{II}PPDME and Cu^{II}PP.

Walker (1974) reported on a low-temperature ESR investigation of Co^{II}TPP frozen glasses in the presence of a variety of π donors and acceptors which produce similar effects as the free-base porphyrin. The spectra yielded unambiguous evidence for the formation of π complexes as characterized by changes in both *g* values and coupling constants. However, since the low-temperature *g* values of the cobalt porphyrins were shown to depend critically on solvent, temperature, and planarity due to axial solvation of the cobalt, even in weak solvents such as chloroform (La Mar & Walker, 1973; Walker, 1970), it was not possible to compare *g* values of Co^{II}TPP in the presence of a substrate without the complication of axial solvation.

Fulton & La Mar (1976a,b) have shown that proton nuclear magnetic resonance can be used successfully to characterize the electronic structure of Co^{II}*p*-MeTPP and that the solution structure at ambient temperature is free from the problems

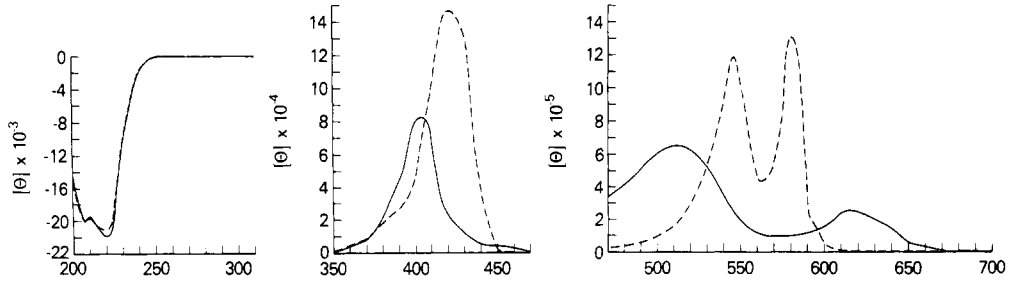

FIGURE 5: Circular dichroism spectra of $Fe^{III}Mb$ (—) and $Cu^{II}Mb$ (---) in H_2O, pH adjusted to 7.0. Protein concentrations were in the micromolarity range.

of axial solvation of the metal and of porphyrin aggregation. The above authors therefore were able to determine, directly by NMR, the effect of π complex formation on the porphyrin chemical shifts. TNB, one of the strongest π acceptors, was used to arrive at a quantitative description of the solution structure of the 1:1 Co^{II}*p*-MeTPP complex. Their analysis showed that the π–π interaction occurs exclusively at the pyrrole parts of the porphyrin ring and does not involve the metal directly. The peripheral π complex exists with an interplanar spacing of 3.2 ± 0.2 Å and the TNB exists over the pyrroles with its center displaced 0.4 ± 0.4 Å from the center of the pyrrole rings toward the cobalt with a proton pointing toward the metal.

The above conclusion is also consistent with other X-ray crystallographically characterized π complexes of TNB for which interplanar spacings in the range of 3.2–3.5 Å are reported (Castellano et al., 1971; Bernstein et al., 1956).

The results in Table IVa show that once the free base is added to Cu^{II}PPDME no significant differences are seen between the noncoordinating chloroform and the coordinating pyridine and piperidine ligands. Since TNB is known to orient itself over the pyrrole rings, it can be reasoned that the free-base porphyrins of the copper derivatives used in our studies orient themselves in the same or a similar way. Also, TNB and the free-base porphyrins are π-acceptor ligands with the free base being the larger of the conjugated systems. Therefore, the predominant effect observed in the interaction of Cu^{II}PPDME with basic ligands in the presence of the free base is believed to be that of the free base. Our results indicate that once separation of the copper porphyrin occurs, it happens in such a way that an extraplanar ligand is blocked from coordinating to the metal center. In Cu^{II}TPP, aggregation is absent due to the configuration of the phenyl rings, and therefore a magnetic interaction between the Cu(II) centers is not expected in the ESR spectrum of Cu^{II}TPP.

The solution ESR spectrum of $Cu^{II}Mb$ at room temperature (Figure 3) has resolvable copper hyperfine components with an average splitting of 178 G. This anisotropic spectrum is the result of the long rotational correlation time of the molecule. No superhyperfine splitting is observed on the copper hyperfine lines, and only a small amount of superhyperfine splitting is seen in the perpendicular region, resulting from the porphyrin nitrogens interacting with the unpaired electron of the Cu(II) atom. $Cu^{II}Mb$ at 77 K (Figure 4) yields the usual copper ESR spectrum with the three hyperfine copper components in the low-field region fairly well separated from each other and the fourth component overlapping with the perpendicular region of the spectrum. On the low-field portion, each of the copper hyperfine components is split into nine lines which are equally spaced by 13 G. The nine lines appear in the intensity ratio of 1:4:10:16:19:16:10:4:1 which indicates the presence of four equivalent nitrogens interacting with the unpaired electron of the copper. The coordinating effect of the fifth ligand is seen in the increase in $g_{\|}$, the decrease in $A_{Cu(\|)}$, and the decrease in the superhyperfine splitting (Table III). The perpendicular part of the spectrum is very complicated but is similar to that of Cu^{II}TPP. In Cu^{II}TPP, as in $Cu^{II}Mb$, there are 15 lines which are equally separated by 16 and 15.5 G, respectively. Splitting of the copper hyperfine components in the parallel region of $Cu^{II}Mb$ is somewhat smaller than the splitting for Cu^{II}TPP and Cu^{II}PPDME, 178 G as compared to 200 G.

Our ESR results clearly show that Cu^{II}PP is complexed with apoMb. The protein offers a high molecular weight environment and prevents porphyrin aggregation, assuring a magnetically dilute spectrum. The ESR results strongly support the UV–vis results that the Cu(II) is five coordinate, in contrast to the octahedral configuration proposed by Andres & Atassi (1970).

CD Studies of $Cu^{II}Mb$ in the Ultraviolet and Visible Region. The ultraviolet and Soret CD spectra of $Fe^{III}Mb$ and $Cu^{II}Mb$ are given in Figure 5. The UV CD spectrum of $Cu^{II}Mb$ is nearly identical with the one reported by Andres & Atassi (1970). In the Soret region the rotation of the $Cu^{II}Mb$ is much larger (14.8×10^4 deg cm^2/dmol) than that of the $Fe^{III}Mb$ (8.33×10^4 deg cm^2/dmol).

The ultraviolet CD spectrum of $Cu^{II}Mb$ clearly shows its globin conformation to be nearly identical with that of $Fe^{III}Mb$ (Figure 5), which is in agreement with the results of Andres & Atassi (1970). Atassi (1967) previously reported the reconstitution of apoMb with iron, manganese, cobalt, nickel, copper, and zinc metalloporphyrins. The immunochemistry of all of these Mb derivatives was investigated to determine if they induced conformational changes which affect the antigen–antibody reaction against antibodies to native myoglobin. It was found that $Cu^{II}Mb$ and reconstituted $Fe^{III}Mb$ reacted the same as native Mb, which indicates that the conformation of the two is identical by Ouchterlony methods. It must be noted that it has not been demonstrated that the antibodies used by Atassi can discriminate between the liganded oxy form of Mb and the unliganded deoxy form.

However, due to the large increase in the rotational strength of the Soret band of $Cu^{II}Mb$ (14.8×10^4) over that of $Fe^{III}Mb$ (8.33×10^4) (Figure 5), a difference in the two myoglobins seems to exist. A similar difference has been observed between deoxy- and oxyMb (ca. 22% decrease) (Hsu & Woody, 1971) and deoxy- and oxyHb (Sugita et al., 1971).

The unliganded metalloporphyrin alone, due to its symmetry, is optically inactive. However, when it is bound to a protein, induced Cotton effects arise from heme–protein interactions. This optical activity can occur in several ways: (a) the porphyrin can be distorted by twisting, such distortion leading to nonvanishing rotational strengths in all transitions, hence, an inherently dissymetric chromophore (Moscowitz, 1961); (b) the five-coordinate square-pyramidal or six-coordinate with different extraplanar ligand MPP's are chiral

at the metal center and thus potentially optically active (Eichhorn, 1961); (c) it may retain a planar geometry, but a chiral electrostatic field, imposed by the binding site of the protein, will cause transitions of differing symmetry to mix together, allowing transitions which are forbidden in the isolated chromophore to acquire magnetic dipole character (Condon et al., 1937); (d) by the coupled oscillator mechanism, whereby an electrically allowed transition (purely linear motion) can couple with transitions in other chromophores (Kirkwood, 1937).

Hsu & Woody (1969, 1971) showed that coupled oscillator interactions between porphyrin $\pi \rightarrow \pi^*$ transitions and the aromatic side chains could account for the sign and magnitude of the observed CD bands in Mb and Hb. Some other types of possible interactions (for example, coupling with peptide $\eta \rightarrow \pi^*$ and $\pi \rightarrow \pi^*$ transitions of the peptide backbone) were ruled out by calculations which showed them to be too small. The possibility that one-electron mixing with the metal d $\rightarrow$ d transitions was excluded by noting that both oxidation and spin-state changes did not drastically alter rotational strength of the heme transitions.

Subsequent work has strengthened the conclusion reached by Hsu & Woody (1969, 1971). For example, the negligible role of mixing between porphyrin $\pi \rightarrow \pi^*$ and metal d $\rightarrow$ d transitions has been demonstrated by the observation that globin complexes with PP, without any iron, have a CD spectrum very similar to that of native hemoglobin (Sugita et al., 1971; Ruckpaul et al., 1970), except for the additional splitting in the visible region due to the lower symmetry of the free-base porphyrin. Additional support has come from CD and X-ray studies of invertebrate Hb (Sugita et al., 1971, 1968; Formanek & Engel, 1968; Huber et al., 1971) where it was shown that the polypeptide chain folding in these hemoglobins is almost identical with that of Mb and the individual chains in mammalian hemoglobins. The reversal in sign of the CD, despite nearly identical conformations, supports the conclusion that coupling with the peptide groups is not significant. However, the distribution and arrangement of the aromatic side chains are quite different, and calculations based on the X-ray structures of Chironomus (Fleischhauer & Wollmer, 1972) and Lamprey hemoglobins (Woody, 1975) have shown that the reversal in sign of the Soret band can be accounted for by the same coupled oscillator interactions postulated for vertebrate heme proteins (Hsu & Woody, 1969, 1971).

Ferrone & Topp (1975) have shown that, on addition of IHP to Fe^{III}Hb at pH 6, the Soret rotational strength increases from 0.13 to 0.28 DBM. The net increase of 0.15 DBM is nearly identical with the increase which occurs on going from oxy- to deoxyHb (0.17 to 0.33 DBM).

Chien & Synder (1976) reported that deoxygenation increases the Soret rotational strength of oxyHb by 95%, and the corresponding increase for Co^{II}Hb was 120%. It was also shown that IHP increases the Soret rotational strength of Co^{II}deoxyHb by about 10% and Co^{III}Hb by about 20%.

Plese & Amma (1977) observed increases in the Soret band of Mn(III)Hb and N_3Mn^{III}Hb in the presence of IHP. There was a large increase in the rotation of the Soret band for Mn^{II}Hb over Mn^{III}Hb, but the effect of IHP on the former was not studied.

In the case of Hb, the rotational strength of the Soret band depends strongly on the intersubunit interactions. The heme group in one subunit interacts with the aromatic groups of neighboring subunits (Hsu & Woody, 1971), and this is probably true for cobalt and manganese Hb as well. Both quaternary and tertiary changes which effect the environment of the heme can bring about changes in the rotational strength of the Soret band. In Mb quaternary changes do not exist, and therefore tertiary changes alone must account for the rotational strength increases.

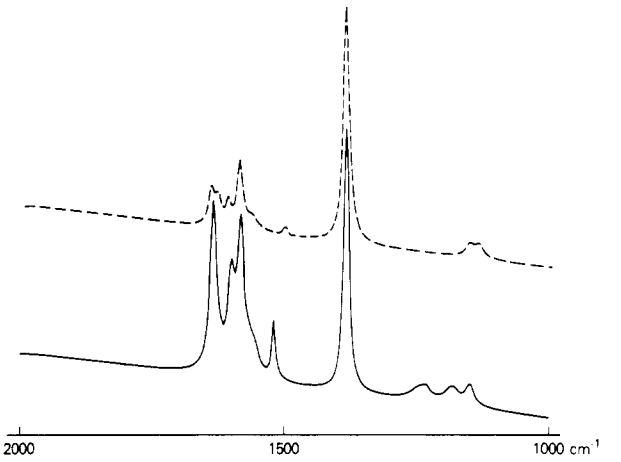

FIGURE 6: Resonance raman spectra of copper(II) protoporphyrin IX myoglobin (---) and copper(II) protoporphyrin IX dimethyl ester (—). Cu^{II}PPMb was run in 0.05 M Mes buffer and 0.05 M KCl, pH 7.0; Cu^{II}PPDME was run in Cs_2. In both cases the concentration was 0.001 M and the 4579-Å exciting line from an argon ion laser was used to obtain the spectra. The spectra were simulated by using the CAP program on a Nicolet 1180 computer using the line frequencies, widths, and intensities reported in Table V. The more complicated areas were analyzed with the aid of a Du Pont curve analyzer.

Table V: Frequencies, Line Widths, and Intensities for the Peaks Used to Simulate the Resonance Raman Spectra Shown in Figure 8

Cu^{II}PPDME			Cu^{II}Mb		
frequency[a]	half band width[a]	intensity[b]	frequency[a]	half band width[a]	intensity[b]
1134	20	16	1120	20	10
1169	33	13	1138	20	10
1219	20	6	1374	14	184
1234	12	9	1498	12	6
1373	12	206	1557	25	9
1503	9	45	1580	15	51
1550	16	14	1603	10	17
1560	15	12	1623	15	20
1578	16	106	1636	13	26
1584	37	8			
1596	16	64			
1634	16	130			

[a] In centimeters^{-1}. [b] In millimeters.

We note that both metMb and oxyMb have nearly identical rotations at the Soret transition (Sugita et al., 1971). In both metMb and oxyMb the iron is in the Fe(III) oxidation state (Yamamoto et al., 1973; Spiro & Strekas, 1974). In deoxyMb, containing the less polar Fe(II), the rotational strength of the Soret band increases. In the Cu^{II}Mb the rotational strength of the Soret band is also much increased over both the met- and deoxyMb. We suggest that the packing of the Mb side chains that affects the rotational strength of the Soret transition is largely controlled by the polarity of the metalloporphyrin.

It has been suggested that the R–T transition in Hb may involve a doming of the porphyrin (Hoard, 1971, 1975; Anderson, 1973), associated with the movement of the iron atom to a point distinctly out of the heme plane. However, Ferrone & Topp (1975) observed no changes in Raman frequencies in the transition induced by IHP binding and only

intensity changes consistent with a small extent of spin-state change. The calculations on the effect of doming predict a sizable contribution but of the wrong sign to account for the increase in Soret rotational strength of the T form (Woody, 1978). Thus, it appears unlikely that distortions in the heme geometry are the source of the increased Soret rotational strength.

Resonance Raman Spectra of $Cu^{II}Mb$ and $Cu^{II}PPDME$. The resonance Raman spectra of $Cu^{II}Mb$ in Mes buffer and $Cu^{II}PPDME$ in CS_2 are shown in Figure 6. The original spectra were analyzed with the aid of a Du Pont curve analyzer and redrawn by using the CAP program on a Nicolet 1180 computer. The frequencies, line widths, and intensities for the peaks used to simulate the resonance Raman spectra are given in Table V.

Resonance Raman spectroscopy has been applied to a variety of metalloporphyrins and heme proteins in attempts to monitor both metal ion oxidation states and porphyrin conformation (Spiro, 1975). There are several reports on resonance Raman studies of copper(II) porphyrins (Verma et al., 1974; Spaulding et al., 1975).

The metalloporphyrin vibrational modes that are prominent in the resonance Raman spectrum are strongly dependent on the excitation frequency. We have chosen for this study the 4579-Å exciting line of an argon ion laser, a frequency close to the Soret transition. For excitation near the Soret transition, totally symmetric vibrational modes are enhanced (Spiro, 1975).

The most prominent band in both the $Cu^{II}PPDME$ and $Cu^{II}Mb$ spectra is at 1374 cm^{-1} and has been assigned to an A_{1g} vibrational mode. This band is used as an oxidation-state marker for iron porphyrins. A similar strong band occurs at 1379 cm^{-1} in $Cu^{II}OEP$ in both the solid state and in solution (Spaulding et al., 1975). The rest of the resonance Raman spectrum of $Cu^{II}PPDME$ and $Cu^{II}Mb$ shows considerable difference in both the number of peaks and relative intensities. There are obviously fewer peaks present in the $Cu^{II}Mb$ spectrum, and the intensity relative to the 1374-cm^{-1} line is less.

The most prominent difference is the moderately intense line at 1503 cm^{-1} in the $Cu^{II}PPDME$ spectrum which is shifted to 1498 cm^{-1} and is much weaker in the $Cu^{II}Mb$ spectrum. A polarized line of moderate intensity is observed in $Cu^{II}OEP$ at 1504–1505 cm^{-1} in both the solid state and in solution. A similar polarized line occurs in nearly all metalloporphyrins in the 1482–1521-cm^{-1} region (Spaulding et al., 1975). Since the position of this line is both structure and oxidation-state dependent, the similarity of position in both the $Cu^{II}PPDME$ and $Cu^{II}Mb$ argues that the conformation of the copper(II) porphyrin is essentially the same in CS_2 solution as in the hydrophobic myoglobin pocket. Shifts in peak positions of 4 cm^{-1} are common in going from the solid state to solution or in changing solvents.

The strong peaks in the 1580–1640-cm^{-1} range seem to have essentially the same position in both the $Cu^{II}PPDME$ and the $Cu^{II}Mb$ spectra. The difference in appearance in this area probably results from changes in intensity of these peaks. The differences in the relative intensitives of the lines in the $Cu^{II}PPDME$ and $Cu^{II}Mb$ spectra could be to some extent due to the shift in the λ_{max} of the Soret peak from 413 to 425 nm on binding the porphyrin to the protein. This limited resonance Raman study, involving only one exciting wavelength, provides no evidence that the copper(II) porphyrin undergoes any significant change in conformation in going from the four-coordinate square-planar solution form to the five-coordinate form in the myoglobin pocket. This is qualitatively similar to results obtained earlier for the binding of several cobalt(II) porphyrins to myoglobin and hemoglobin (Woodruff et al., 1975).

Concluding Discussion. Atassi (1967) first prepared $Cu^{II}Mb$ and demonstrated by quantitative analysis of the copper content that one $Cu^{II}PP$ was bound per globin. He also determined (Andres & Atassi, 1970) that the UV CD spectrum is nearly identical with that of $Fe^{III}Mb$, implying that the conformation of the protein is very similar in both cases. It has been further observed that the immunochemistry (Atassi, 1967) of $Cu^{II}Mb$ and $Fe^{III}Mb$ is identical.

Our results support Atassi's basic findings and extend them in several new directions. The Soret and visible transitions of the $Cu^{II}PP$ are strongly supportive of the $Cu^{II}PP$ being five coordinate in the heme pocket. The well resolved ESR spectrum of the $Cu^{II}Mb$ requires that the $Cu^{II}PP$ be magnetically dilute and is also strongly supportive of the $Cu^{II}PP$ being specifically bound at the heme pocket. The g values and the hyperfine coupling values reported are consistent with a five-coordinate $Cu^{II}PP$, supporting the Soret and visible results. The Soret and visible CD results show a considerable difference between $Cu^{II}Mb$ and $Fe^{III}Mb$, which we ascribe to differences in the packing of the amino acid side chains around the porphyrin in the heme pocket. Studies currently under way on the denaturation of $Cu^{II}Mb$ support this interpretation and will be reported in full in the near future. The resonance Raman studies show little distortion of the $Cu^{II}PP$ in going from solution into the heme pocket.

It is interesting to compare the results reported here for $Cu^{II}Mb$ to those reported for copper(II) cytochrome *c* (Findlay et al., 1977). In the case of copper(II) cytochrome *c*, the Soret band was shifted 24 nm from $Cu^{II}MesoDME$, strongly suggesting that the Cu(II) center is six coordinate as it is in the native cytochrome *c*. The ESR parameters reported for copper(II) cytochrome *c* are very similar to those reported in this paper for $Cu^{II}Mb$. One would not expect a large dependence of the ESR parameters on a weak tetragonal field.

It appears that $Cu^{II}PP$ has many useful spectroscopic properties for exploitation as a reporter group of the heme environment in heme proteins. In $Cu^{II}Mb$ it is five coordinate and not appreciably distorted from its square-planar solution conformation. The globin conformation is very similar to that in $Fe^{III}Mb$, but the packing of the amino acid residues around the porphyrin is different.

Acknowledgments

We are grateful to Professor T. G. Spiro and Dr. J. Stong of Princeton University and Professor G. Walrafen of Howard University for the resonance Raman spectra and to Dr. H. Kon of the National Institutes of Health for many helpful discussions.

References

Adler, A. D. (1967) *J. Org. Chem. 32*, 476.
Anderson, L. (1973) *J. Mol. Biol. 79*, 495–506.
Andres, S. F., & Atassi, M. Z. (1970) *Biochemistry* 9, 2268–2275.
Antonini, E., & Brunori, M. (1971) *Hemoglobin and Myoglobin in Their Reactons with Ligands*, pp 43–107, North-Holland Publishing Co., Amsterdam.
Asakura, T., Leigh, J. S., Drott, H. R., Yonetaoni, T., & Chance, B. (1971) *Proc. Natl. Acad. Sci. U.S.A. 68*, 861–865.
Assour, J. M. (1965) *J. Chem. Phys. 43*, 2477–2489.

Atassi, M. Z. (1967) *Biochem. J. 103*, 29–35.
Baker, E. W., Corwin, A. H., & Whitten, D. G. (1963a) *J. Am. Chem. Soc. 85*, 3621–2624.
Baker, E. W., Whitten, D. G., & Corwin, A. H. (1963b) *J. Org. Chem. 28*, 2363–2368.
Baker, E. W., Brookhart, M. S., & Corwin, A. H. (1964) *J. Am. Chem. Soc. 86*, 4587–4590.
Baker, E. W., Storm, C. B., McGrew, G. T., & Corwin, A. H. (1973) *Bioinorg. Chem. 3*, 49–60.
Barnett, G. H., Hudson, M. F., & Smith, K. M. (1973) *Tetrahedron Lett. 30*, 2887–2888.
Bernstein, H. J., Schneider, W. G., & Pople, J. A. (1956) *Proc. R. Soc. London, Ser. A 236*, 515–528.
Breslow, E. (1964) *J. Biol. Chem. 239*, 486–496.
Breslow, E., & Gurd, F. R. N. (1963) *J. Biol. Chem. 238*, 1332–1342.
Bryce, G. F. (1966) *J. Phys. Chem. 70*, 3549–3557.
Castellano, E. E., Hodder, J. R., Prout, C. K., & Sadler, P. J. (1971) *J. Chem. Soc. A*, 2620–2627.
Chein, J. C., & Snyder, F. W. (1976) *J. Biol. Chem. 251*, 1670–1674.
Chien, J. C., & Dickinson, L. C. (1972) *Proc. Natl. Acad. Sci. U.S.A. 69*, 2783–2787.
Clark, J. F., & Gurd, F. R. N. (1967) *J. Biol. Chem. 242*, 3257–3264.
Condon, E. U., Altar, W., & Eyring, H. (1937) *J. Chem. Phys. 5*, 753–755.
Eichhorn, G. L. (1961) *Tetrahedron 13*, 208–218.
Falk, J. E. (1964) in *Porphyrins and Metalloporphyrins*, Elsevier, Amsterdam.
Ferrone, F. A., & Topp, W. C. (1975) *Biochem. Biophys. Res. Commun. 66*, 444–450.
Findlay, M. C., Dickinson, K. C., & Chien, J. C. W. (1977) *J. Am. Chem. Soc. 99*, 5168–5173.
Fleischhauer, J., & Wollmer, A. (1972) *Z. Naturforsch., B 27*, 530–532.
Formanek, H., & Engel, J. (1968) *Biochim. Biophys. Acta 160*, 151–158.
Fulton, G. P., & La Mar, G. N. (1976a) *J. Am. Chem. Soc. 98*, 2119–2124.
Fulton, G. P., & La Mar, G. N. (1976b) *J. Am. Chem. Soc. 98*, 2124–2128.
Gouterman, M. (1959) *J. Chem. Phys. 30*, 1139–1161.
Gouterman, M. (1978) in *The Porphyrins* (Dolphin, D., Ed.) Academic Press, New York.
Gouterman, M., Schwarz, F. P., Smith, P. D., & Dolphin, D. (1973) *J. Chem. Phys. 59*, 676–690.
Grinstein, M. (1947) *J. Biol. Chem. 167*, 515–519.
Hardman, K. D., Eylar, E. H., Ray, D. K., Banaszak, L. J., & Gurd, F. R. N. (1966) *J. Biol. Chem. 241*, 432–442.
Hoard, J. L. (1971) *Science 175*, 1295–1302.
Hoard, J. L. (1975) in *Porphyrins and Metalloporphyrins* (Smith, E. D., Ed.) pp 317–376, Elsevier Scientific, New York.
Hoffman, B. M. (1975) *J. Am. Chem. Soc. 97*, 1688–1693.
Hoffman, B. M., & Petering, D. H. (1970) *Proc. Natl. Acad. Sci. U.S.A. 67*, 637–643.
Hoffman, B. M., & Gibson, Q. H. (1978) *Proc. Natl. Acad. Sci. U.S.A. 75*, 21–25.
Hoffman, B. M., Spilburg, C. A., & Petering, D. H. (1971) *Cold Spring Harbor Symp. Quant. Biol. 36*, 343–348.
Horrocks, W. DeW., Jr., Veteicher, R. F., Spillburg, C. A., & Vallee, B. L. (1975) *Biochem. Biophys. Res. Commun. 64*, 317–322.
Hsu, M. C., & Woody, R. W. (1969) *J. Am. Chem. Soc. 91*, 3679–3681.
Hsu, M. C., & Woody, R. W. (1971) *J. Am. Chem. Soc. 93*, 3515–3525.
Huber, R., Epp, O., Steigemann, W., & Formanek, H. (1971) *Eur. J. Biochem. 19*, 42–50.
Jones, W. C., Rothgeb, T. M., & Gurd, F. R. N. (1976) *J. Biol. Chem. 251*, 7452–7460.
Kirkwood, J. G. (1937) *J. Chem. Phys. 5*, 479–491.
La Mar, G. N., & Walker, F. A. (1973) *J. Am. Chem. Soc. 95*, 1790–1796.
MacCragh, A., Storm, C. B., & Koski, W. S. (1965) *J. Am. Soc. 87*, 1470–1476.
Manoharan, P. T., & Rogers, M. T. (1969) in *ESR of Metal Complexes* (Yen, T. F., Ed.) pp 143–173, Plenum Press, New York.
McGarvey, B. R. (1956) *J. Phys. Chem. 60*, 71–76.
Miller, J. R., & Dorough, G. D. (1952) *J. Am. Chem. Soc. 74*, 3977–3981.
Moscowitz, A. (1961) *Tetrahedron 13*, 48–56.
Nappa, M., & Valentine, J. S. (1978) *J. Am. Chem. Soc. 100*, 5075–5080.
Penke, B., Feremz, R., & Kovais, K. (1974) *Anal. Biochem. 60*, 45–50.
Plese, C. F., & Amma, E. L. (1977) *Biochem. Biophys. Res. Commun. 77*, 837–844.
Ruckpaul, K., Rein, H., & Jung, F. (1970) *Naturwissenschaften 57*, 131–132.
Spauling, L. D., Chang, C. C., Yu, N.-T., & Felton, R. H. (1975) *J. Am. Chem. Soc. 97*, 2517–2525.
Spiro, T. G. (1975) *Biochim. Biophys. Acta 416*, 169–189.
Spiro, T. G., & Strekas, T. C. (1974) *J. Am. Chem. Soc. 96*, 338–345.
Stryer, L. (1965) *J. Mol. Biol. 13*, 482–495.
Sugita, Y., Dohi, Y., & Yoneyama, Y. (1968) *Biochem. Biophys. Res. Commun. 31*, 447–452.
Sugita, Y., Nagai, M., & Yoneyama, Y. (1971) *J. Biol. Chem. 246*, 383–388.
Swartz, H. M., Bolton, J. R., & Borg, D. C. (1972) in *Biological Application of Electron Spin Resonance*, p 125, Wiley-Interscience, New York.
Teale, F. W. J. (1959) *Biochim. Biophys. Acta 35*, 543.
Verma, A. L., Mendelsohn, R., & Bernstein, H. J. (1974) *J. Chem. Phys. 61*, 383–390.
Walker, F. A. (1970) *J. Am. Chem. Soc. 92*, 4235–4244.
Walker, F. A. (1974) *J. Magn. Reson. 15*, 201–206.
Woodruff, W. H., Adams, D. H., Spiro, T. G., & Yonetani, T. (1975) *J. Am. Chem. Soc. 97*, 1695–1698.
Woody, R. W. (1975) in *Protein-Ligand Interactions* (Sund, H., & Glauer, G., Eds.) pp 60–77, Walter de Gruyter, Berlin.
Woody, R. W. (1978) in *Biochemical and Clinical Aspects of Hemoglobin Abnormalities* (Caughey, W. S., Ed.) 279–298, Academic Press, New York.
Yamamoto, T., Palmer, G., Gilld, D., Salmeen, I. T., & Rimai, L. (1973) *J. Biol. Chem. 248*, 5211–5213.
Yamamoto, H., Kayne, F. J., & Yonetani, T. (1974) *J. Biol. Chem. 249*, 691–698.
Yonetani, T., & Scrivastaua, T. S. (1974) *Fed Proc., Fed. Am. Soc. Exp. Biol. 33*, 1449–1450.
Yonetani, T., Yamamoto, H., & Woodrow, G. V. (1974) *J. Biol. Chem. 249*, 682–690.